

Monitoring land subsidence in Yangon, Myanmar using Sentinel-1 persistent scatterer interferometry and assessment of driving mechanisms

van der Horst, Teije; Rutten, Martine M.; van de Giesen, Nick C.; Hanssen, Ramon F.

DOI

[10.1016/j.rse.2018.08.004](https://doi.org/10.1016/j.rse.2018.08.004)

Publication date

2018

Document Version

Final published version

Published in

Remote Sensing of Environment

Citation (APA)

van der Horst, T., Rutten, M. M., van de Giesen, N. C., & Hanssen, R. F. (2018). Monitoring land subsidence in Yangon, Myanmar using Sentinel-1 persistent scatterer interferometry and assessment of driving mechanisms. *Remote Sensing of Environment*, 217, 101-110.
<https://doi.org/10.1016/j.rse.2018.08.004>

Important note

To cite this publication, please use the final published version (if applicable).
Please check the document version above.

Copyright

Other than for strictly personal use, it is not permitted to download, forward or distribute the text or part of it, without the consent of the author(s) and/or copyright holder(s), unless the work is under an open content license such as Creative Commons.

Takedown policy

Please contact us and provide details if you believe this document breaches copyrights.
We will remove access to the work immediately and investigate your claim.

Green Open Access added to TU Delft Institutional Repository

'You share, we take care!' – Taverne project

<https://www.openaccess.nl/en/you-share-we-take-care>

Otherwise as indicated in the copyright section: the publisher is the copyright holder of this work and the author uses the Dutch legislation to make this work public.



Monitoring land subsidence in Yangon, Myanmar using Sentinel-1 persistent scatterer interferometry and assessment of driving mechanisms

Teije van der Horst, Martine M. Rutten, Nick C. van de Giesen, Ramon F. Hanssen*

Delft University of Technology, Stevinweg 1, Delft 2628 CN, The Netherlands

ARTICLE INFO

Keywords:

Subsidence
Yangon
Sentinel-1
Groundwater
PSI
InSAR

ABSTRACT

Inhabitants and ecosystems in delta areas are becoming increasingly vulnerable to the effects of subsidence, caused by anthropogenic activities. Yangon is a city on the periphery of the Irrawaddy delta in Myanmar where little is known about the true extent of this hazard, while its effects can potentially harm millions of its inhabitants. This research presents the magnitude and extent of the subsidence hazard in Yangon through a Persistent Scatterer Interferometry (PSI) time-series analysis on the Sentinel-1 data archives in the period of December 2015 through April 2017. The PSI analysis revealed four distinct zones of varying sizes where vertical velocity differences over 20 mm/yr were found, locally exceeding 110 mm/yr. The significant subsidence zones are exclusively located in young Alluvium deposits and 95% of velocity differences over 10 mm/yr are found at Quaternary age deposits. The addition of loads, such as buildings, predominantly affect subsidence rates in the first decade after placement. Estimates of groundwater extraction for domestic supply, used by more than 2 million inhabitants, correlate with the township average subsidence rates which shows that most subsidence in Yangon can be explained by groundwater extraction. Current operation of groundwater extraction wells induces an aquifer volume loss of 5.5 million cubic meter per year in the aquifer system of Yangon city. Unless groundwater extractions are mitigated, Yangon will be increasingly vulnerable to infrastructural damages, flooding events, and degrading aquifer quality.

1. Introduction

Many delta areas in the world are experiencing the consequences from subsiding land surface (Syvitski, 2008). Human-induced land subsidence is mainly caused by extraction of resources from the subsoil, such as groundwater and hydrocarbons, and can outpace natural subsidence or sea-level rise by one or two orders of magnitude (Higgins, 2015; Minderhoud et al., 2017). Among the problems resulting from subsidence are an increased vulnerability to flooding events, infrastructural damages or failures, and permanent geological deformation (Syvitski et al., 2009; Wang et al., 2013). Deltas that accommodate mega-cities in Asia are especially affected, as large populations and rapid urban growth development have profound impacts on their environment (Syvitski et al., 2009).

Yangon city is an example of such a delta city where 5 million inhabitants are confronted with the negative effects of groundwater extraction such as seen in cities such as Bangkok (Phien-wej et al., 2006), Shanghai (Chai et al., 2004), the Hong Kong surroundings (Chen et al., 2012), and Ho Chi Minh City (Thoang and Giao, 2015). In Yangon City, groundwater is the most significant source of water supply (JICA,

2014b) which means that subsidence can be expected. Although the potential for subsidence has been reported before (RVO Netherlands, 2014), until now no preventive or even monitoring measures have been taken (Aobpaet et al., 2014; personal communication surveying department, 31 July 2017).

Subsidence is usually caused by compaction of aquitards through an increase in effective stress. An increase in effective stress in the soil skeleton follows from drawdown of the water table or an addition of load on top of the soil. This results in elastic strain, inelastic strain, and consolidation of compressible layers for effective stresses larger than the historical stress (Galloway et al., 1998; Verruijt, 2012). The major part of the fine-grained silt and clay layer compaction is an irreversible rearrangement of the pore structure while a significantly smaller elastic strain rebounds after recovery of the initial groundwater level (Motagh et al., 2017). The severity and irreparable nature of the consequences of subsidence essentially require monitoring and mitigation for sustainable development.

Satellite based Interferometric Synthetic Aperture Radar (InSAR) has shown great capability in detecting and monitoring subsidence hazards over the past decades, especially when applied with a

* Corresponding author.

E-mail address: R.F.Hanssen@tudelft.nl (R.F. Hanssen).

<https://doi.org/10.1016/j.rse.2018.08.004>

Received 5 March 2018; Received in revised form 30 July 2018; Accepted 5 August 2018

Available online 14 August 2018

0034-4257/ © 2018 Elsevier Inc. All rights reserved.

Persistent Scatterer (PS) time-series analysis (Ferretti et al., 2000, 2001; Hanssen, 2001; Hooper et al., 2012; Van Leijen, 2014). This technique enables the monitoring of large-scale deformation patterns at sub-centimeter precision on a very dense grid (Ferretti et al., 2001; Sousa et al., 2011). The new Sentinel-1 (S1) satellites which are systematically observing the Earth's surface, offer valuable data for deformation monitoring (Berger et al., 2012). They provide C-band data continuity at a swath width of 250 km for the main acquisition mode (Wegmuller et al., 2015). The data is provided free of charge and the sensor system repeat time of 6 days greatly improves the temporal coverage with respect to alternative datasets in the scientific community.

The use of InSAR, in particular Persistent Scatterer Interferometry (PSI) time-series, is especially useful in areas such as Yangon, where other means of monitoring subsidence have never been employed. Aobpaet et al. (2014) show that InSAR-derived vertical velocities can be extracted at the vast majority of the city extent, and that there are velocity differences of several centimeters per year within the city limits in the period of November 2012 until April 2014. The number of used images in this research was enough to identify a network of PS measurement points, but as only 16 Radarsat-2 images—acquired in the dry season—were used, the reliability of the results could be significantly improved. An update of the surface deformation using the S1 datasets is necessary to show the most recent and accurate situation regarding subsidence in Yangon City.

This research presents the results of a PSI analysis applied on Yangon city to assess recent surface deformation using S1. The aim is to detect subsidence areas and identify the most likely driving mechanisms.

2. Study area

Yangon, or Rangoon, shown in Fig. 1 is the old capital and the largest city in Myanmar in terms of population and urbanized area. An estimated 5.2 million people currently inhabit the urbanized area of Yangon region, and this number is expanding with more than 20% each decade (Department of Population, 2015). The same expansion rate is also observed in the extent of the city's urban environment (Morley, 2013).

The city of Yangon requires sufficient inhabitable area for its increasing population. The population density increased by building more high-rise buildings in existing urban areas. Spatial limits of the city were extended by creating new urban land, which can be easily observed from historic Google Earth optical imagery. Agricultural land, mostly flooded for half of the year, is replaced by impervious plots, improved drainage, and external loads of housing, industrial sites, and roads. The decrease of the phreatic surface level, and the addition of loads on the soil lead to an increase in effective soil stress, locally exceeding historic values. This triggers consolidation of the layers beneath, eventually leading to subsidence.

Water supply in Yangon city is partially managed by the Yangon City Development Council (YCDC), responsible for water supply, which supplies less than half of the city with reservoir water via pipes. The other inhabitants rely on private or shared water supply consisting mostly of tube wells (YCDC, 2015) that account for the major part of the groundwater extraction in Yangon. Moreover, many inhabitants who receive water supply via pipes, occasionally also extract groundwater during periods of unavailable reservoir water as the supply availability varies between 6 and 24 h across the city (JICA, 2014b). Additionally, the YCDC extracts water from the ground for 10% of their total water supply (Mon et al., 2013). Finally, water is extracted for industrial

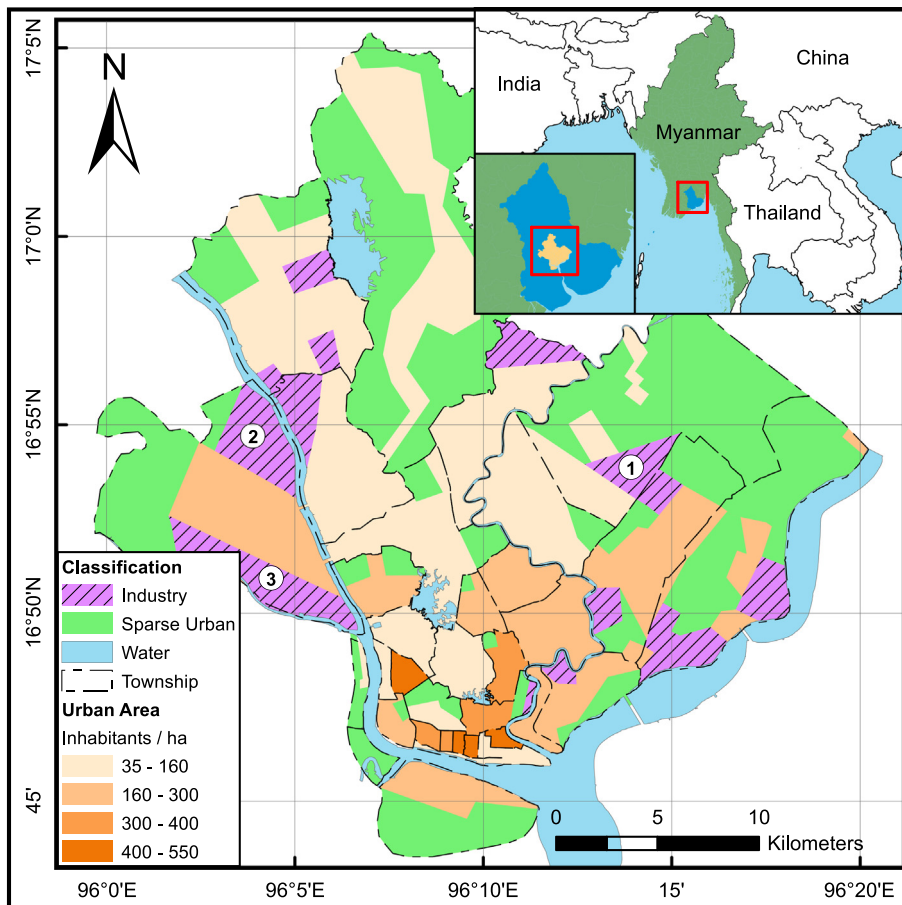


Fig. 1. The top right shows the location of Myanmar and the outline of Yangon city within the Yangon Region. On the left, a map of the study area—Yangon City—showing its 33 townships classified into industrial zones, sparsely urbanized areas with low population density, and urban areas colored by population density. Labels 1 through 3 refer to the industrial zones in Fig. 4. The land-use classification was manually derived from optical satellite imagery.

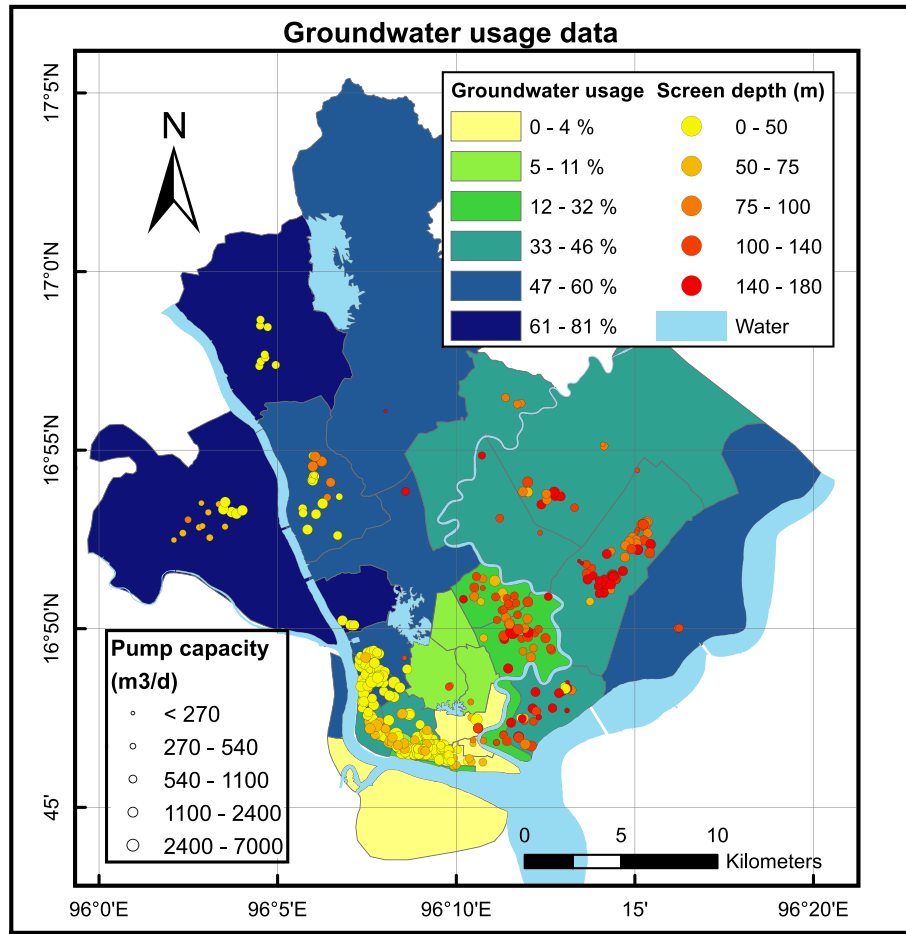


Fig. 2. The data on which the groundwater extraction estimates were based, i.e. the YCDC-managed tube wells' screen depth where the size of each dot represents the extraction capacity, varying between 40 and 7000 m³/d. The color of each township represents the estimated percentage of inhabitants using a private tube well.

usage, for which no data sources were available (personal communication Ministry of Construction, 15 August 2017). Based on these reports, at least 2 million and up to 3 million (JICA, 2014b) inhabitants rely on groundwater extracted from Yangon's aquifers. Reported consequences from these extractions include salt water intrusion (Htun, 2015) and the risk of depletion and subsidence (JICA, 2014b). Policy to eliminate groundwater extractions in 2025 are in place (JICA, 2014a), but these plans are very ambitious and do not refer to private extractions.

Yangon has a tropical savanna climate with distinct wet and dry seasons of relatively equal duration. Most of the annual precipitation falls between May and October while less than 5% precipitates between November and April. On average, 2800 mm of rain per year falls in Yangon city with over 600 mm in the wettest month July. In the monsoon seasons, the heavy rainfall has led to many pluvial flooding events (JICA, 2014c).

3. Materials and methods

3.1. Sentinel-1 PSI time-series

A single master stack of differential interferograms was created in preparation for the PSI analysis. The complete set of 33 ascending Synthetic Aperture Radar (SAR) images from S1, acquired over the city of Yangon between 14 December 2014 and 14 April 2017, was obtained. At first, the images were separated by 24 days until the S1-b satellite started its acquisitions in February 2017 thereby reducing the temporal separation between acquisitions to 12 days. All images were

resampled to the master date, 5 August 2016. The image acquisition time was 11:46 UTC (18:16 local time).

The extraction of a surface deformation signal from the single master stack of interferograms was performed using PSI time-series analysis (Van Leijen, 2014). This technique identifies pixels containing a dominant scatterer, as these are less likely to be affected by decorrelation (Ferretti et al., 2001). The interferometric phase of the selected pixels, referred to as PS, is then used to estimate relative deformations, elevations, as well as the integer phase ambiguities (Hanssen, 2001). A temporally smooth deformation pattern was assumed to constrain the parameter estimation (Kampes, 2005). The interferometric parameter estimation was performed using Antares, an adapted version of the Delft Persistent Scatterer Interferometry (DePSI) software which was developed by Van Leijen (2014). In the following, the deformation observed in the Line of Sight (LoS) to the satellite was projected to the vertical. This facilitates easy interpretation, acknowledging that potential horizontal deformations may introduce a small error in the vertical rates. To assess the impact of this error, the sensitivity to horizontal motion was calculated. The InSAR measurement d_{LOS} is the projection of vertical motion d_u and horizontal motion in the azimuth look direction (ALD) d_{hALD} . Using the relation (Hanssen, 2001):

$$d_{LOS} = d_u \cos(\theta_i) - d_{hALD} \sin(\theta_i), \quad (1)$$

and an incidence angle θ_i of 40°, we find that the sensitivity vector is given by $[0.77, 0.64][d_u, d_{hALD}]^T$, which means that horizontal deformation in the ALD will be erroneously projected onto the vertical, scaled by a factor of 0.83. With a maximum horizontal deformation of 30% of the vertical deformation at the edges of the subsidence bowls,

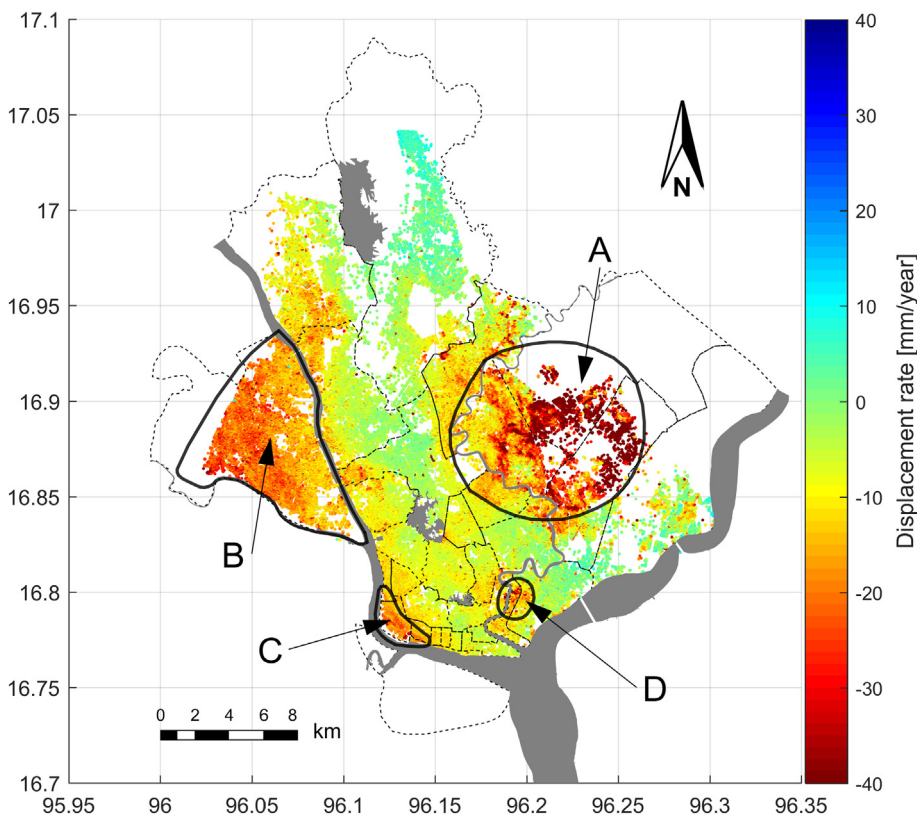


Fig. 3. Annual vertical displacement rate for the S1 ascending orbit. Red and green points indicate downward and stable movement respectively. Gray shapes delineate water bodies in this figure. Four sites of interest with velocity magnitudes over 20 mm/yr are marked with letters A–D for further discussion. Note that the colorbar magnitude limits are constrained to 40 mm/yr. At site A this range is exceeded by 2% of all PS points.

cf. Kratzsch (2012), Samiei-Esfahany et al. (2010) —but likely significantly less—the error in the reported vertical will be less than 25%. For any direction of horizontal motion other than the ALD, this factor is lower and drops to zero at the sensor's heading direction.

3.2. City expansion

The significance of subsidence due to consolidating layers was analyzed by plotting the PS velocities versus the years of construction of the measured objects. The latter were estimated using historic Landsat images from 1984 until 2017 that were accessed through Google Earth (Google, 2017). Polygons were drawn over constructed buildings in the city for each epoch of 1 year. Then, all deformation velocities of PS inside these polygons were extracted for each epoch.

It was possible to reconstruct the development of individual buildings only from 2003 onwards, as the spatial and temporal resolutions used before this year were too coarse and made this approach impossible. Three industrial zones (see Fig. 1) located in deformation hot-spots were mapped using this technique because they were recently constructed and contain many PS per building.

3.3. Water resources

The comparison of subsidence and groundwater levels in the underlying aquifer system has been successfully used in previous research to identify the strong correlation between the two (Galloway et al., 1998; Chai et al., 2004; Ketelaar, 2009). Groundwater level measurements are presently not performed by any governmental organization or research institute in Yangon City (personal communication YCDC). Therefore, subsidence was related to the estimation of volumetric groundwater extractions as will be explained in the next paragraphs.

The assessment on the use of groundwater resources was based on estimates of extraction from private and YCDC-managed tube wells. The private tube well extractions were estimated by JICA (2014b, p. 74) and the YCDC coverage of piped water supply (YCDC, 2015) listing (i) water

supply by source; (ii) water supply coverage rates; and (iii) percentage of city council managed supply of water per township. These reports were combined to estimate the percentage of inhabitants that has private groundwater supply, shown on a map in Fig. 2. The private groundwater extraction volume per township was then estimated by multiplying the number of inhabitants of each township by the percentage estimated private groundwater extraction and a water demand of 125 L per person per day.

To estimate the extraction of the YCDC-managed tube wells, an updated dataset containing 434 operational tube wells was obtained from the YCDC. For each well, the location, capacity, extraction depth and several other parameters were processed. The depth and capacity of these wells are also shown in Fig. 2.

Finally, the extraction volumes were normalized per urbanized area to arrive at specific discharge per township, q_n . This was compared to an estimate of the recharge flux to assess the subsidence potential based on a simple water balance:

$$dS/dt = P_e(1 - k_s) - q_n, \quad (2)$$

with the storage S , the effective rainfall P_e , and the estimated runoff coefficient k_s .

3.4. Geology

The geological formations of Yangon can be used to interpret current subsidence rates. A Quaternary geology map (Naing, 1972) with a description of the general lithology was compared to the deformation results. We expect the thickness of Quaternary deposits to correlate with the potential for subsidence, as they consist generally of unconsolidated soils.

3.5. Site visit and interviews

Over the course of this research, we visited Yangon City to collect data, perform site visits, and contact local authorities. During the visits

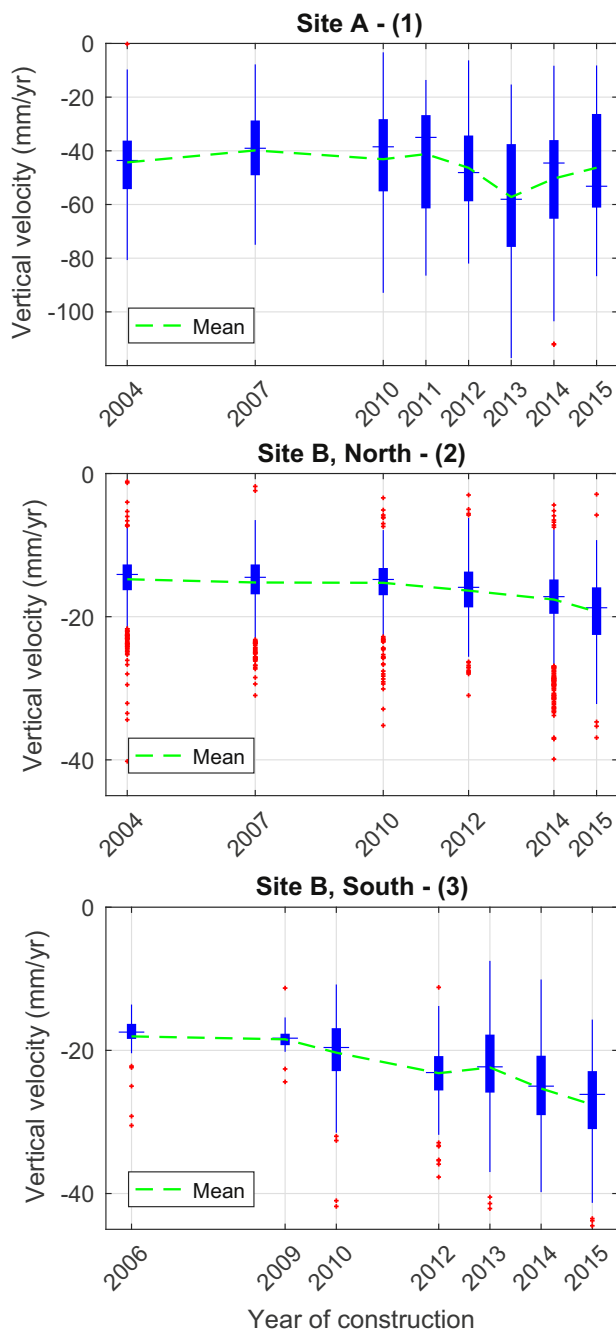


Fig. 4. Boxplots for the industrial zones at sites A and B showing the PSI vertical displacement rates versus the construction date of the measured objects. The number in the title refers to the location in Fig. 1. The wide part of each boxplot shows the interquartile range, the narrow part shows the data range without outliers, and the red crosses denote outliers. The site notations correspond with Fig. 3. Recently placed structures move down more rapidly than structures placed longer ago. Ten years after the placement of the structures, the effect of load onto the surface seems negligible in comparison to the total deformation velocities.

to the YCDC, the Ministry of Construction, the Survey department, the Yangon Technological University (YTU), and Dagon University, we presented our subsidence estimates and the potential driving mechanisms. It showed that there is no unique interpretation on the causes of subsidence for Yangon City. The site visits to subsiding areas were focused especially on possible traces of subsidence and differences in deformation between constructions and the surface.

4. Results

4.1. PSI results

Fig. 3 illustrates the surface deformation map with relative deformation rates measured at roughly 200,000 PS in Yangon city from December 2014 until April 2017 with an average point density of 500/km². The maximum deformation velocity difference over Yangon is 120 mm/yr. The velocity mode is -10 mm/yr which is exceeded in magnitude by 50% of the data. Subsidence rates higher than -20, -30, and -40 mm/yr are found at 15%, 4.5%, and 2% of the PSs, respectively. While the InSAR deformations are inherently relative, the scale of displacement velocities is set to zero at 96.1299°E and 16.8776°N, which is situated over consolidated deposits and has very little groundwater extractions nearby. Spatially integrating these subsidence rates yields an aquifer storage volume loss of 5.5 Mm³/yr representing the void space lost in the subsoil because of compacting layers. The mean of the root mean square errors between the steady-state deformation model and the unwrapped results was found to be 3.5 mm/yr, which is small enough to sustain the hypothesis of steady-state deformation.

The locations where vertical velocity differences greater than 10 mm/yr were found, have been marked with letters A through D for further discussion. The most deforming area, A, covers the Dagon Myothit North, East, and South townships, with deformation rates ranging from -110 to -20 mm/yr. The spatial variation of deformation rates in this area is high compared to the rest of the city. Area B covers the entire Hlaingtharya township and shows a more even distribution of deformation velocities between -10 and -20 mm/yr. Similar rates were found at the sites of C and D which point to the Ahlone and Dawbon townships respectively.

4.2. City expansion

For three industrial zones in Yangon city, the year of construction was mapped against the rate of vertical displacement. Fig. 4 shows three boxplots where the age of construction of the individual buildings is set out against the vertical deformation velocity. These velocities were extracted from the PSI results using roughly 700 polygons that covered constructions built in a certain year. Even though the individual load of constructions is unaccounted for in this analysis, the average deformation of a site is expected to show the system's response.

The most recently constructed buildings are moving down more rapidly than the older ones, as one would expect. The average decreasing velocity magnitude over the number of years since construction can be associated with the process of consolidation and was observed in both industrial zones at site B. The velocity peak observed at constructions placed in 2013 at site A was caused by local effects not associated with construction time. At all sites, the vertical deformation rates found at constructions placed in 2004 show an annual relative difference in subsidence velocity which is less than 2%. Therefore, the effect of additional loads on the surface on the total velocity rate is assumed to be negligible after a period of 10 years.

4.3. Water resources

The used groundwater data, the estimate of extraction, and the estimated change in storage are presented in Fig. 2. Varying between townships, up to 81% of the population uses groundwater extracted by private wells. It is least in the old city center, just north of the river bank in between sites C and D, where the coverage by the YCDC-piped reservoir water is very high, and the supply throughout the day is guaranteed (JICA, 2014b). All other townships have fewer connections and poor service coverage, especially across river banks at sites A and B where most inhabitants rely on private water supply. In the most southern township below the river (Dala) there is no connection to

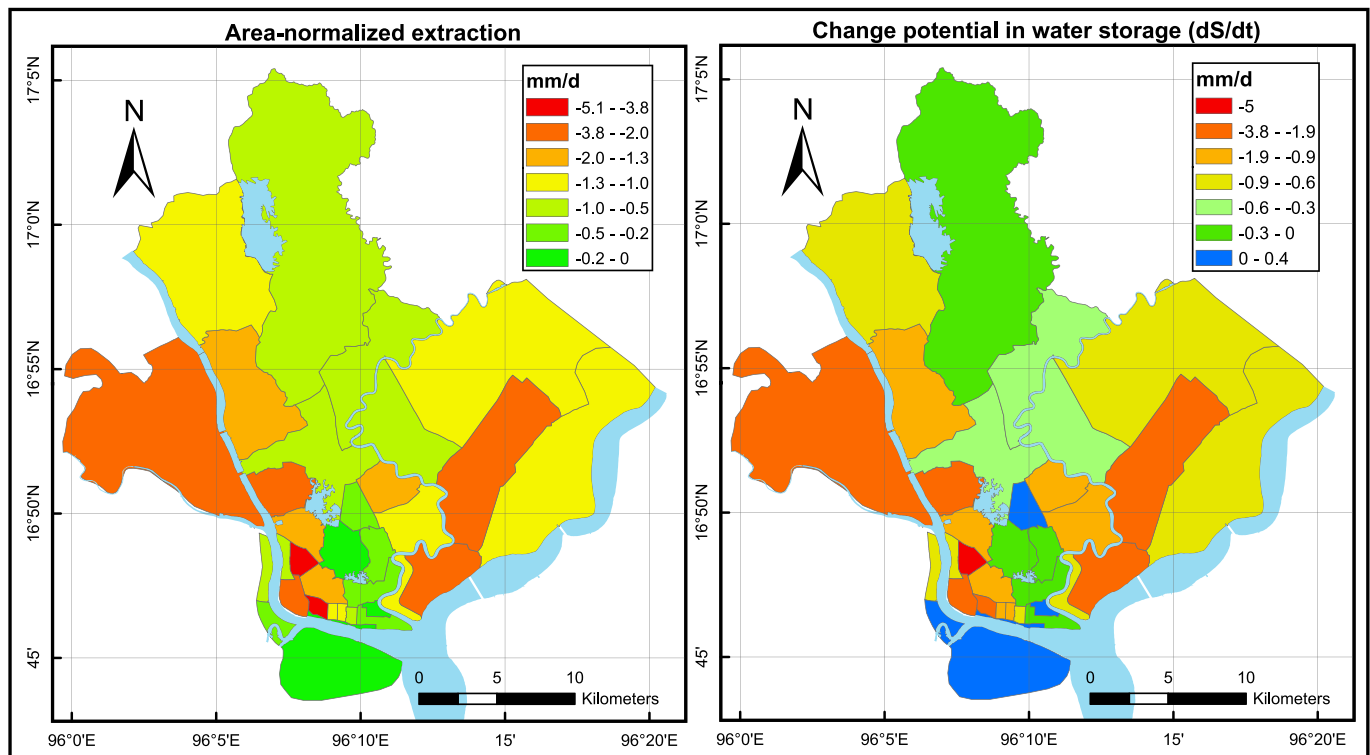


Fig. 5. The left map shows area-normalized groundwater extraction rates constrained by the assumption that YCDC only extracts water for the townships in which the pumps were located and also extracts a small amount of groundwater for areas with high service coverage. Furthermore the extraction was normalized only by the inhabited area of each township. On the right, the difference in vertical water storage of each township that was determined using Eq. (2).

pipled water which is mostly resolved by the usage of surface water rather than the usage of groundwater.

The YCDC-managed tube wells show extraction capacities ranging from 40 to 7000 m³/d and an average capacity of 650 m³/d. As these data show capacity rather than the actual extracted amount, the interpretation of these values needs to be done with caution, especially given the remarkably high density of extraction wells in several townships, which has a combined capacity far greater than the rate of supply. In fact, the combined tube well capacity sums up to three times the reported groundwater extraction of 91,000 m³/d (JICA, 2014b; Htun, 2015). Thus, an operation for all wells of 8 h per day results in an equivalent extraction. The screen depth of the tube wells is divided into an average of 45 m in the west and 125 m in the east of the city.

The extraction map shown on the left of Fig. 5 shows the groundwater extraction estimation for both private extraction wells and YCDC wells combined, normalized over inhabited area. The values of this extraction range from 0 to −5.1 mm/d. The original scenario—in which all YCDC wells extract an 8 h per day equivalent of the full capacity—locally results in extremely high estimates for groundwater extraction. Therefore, a different scenario was adopted in which two constraints were added to simulate the operation of the tube wells more accurately. First, the wells only supply for the inhabitants in the same township. Second, areas well covered (> 95%) by piped reservoir water with a 24 h daily supply only require wells for downtime, estimated at 5% of their capacity.

The right map of Fig. 5 shows the vertical change in aquifer storage calculated with Eq. (2) under the assumption of no horizontal flow. Note that the storage is considered over the full vertical column. The yellow through red values indicate moderate to high change in storage with extraction rates far greater than the recharge rates. These numbers should not be interpreted as actual change in storage, but rather as indicators of subsidence potential.

5. Discussion

5.1. Comments on deformation values

The relative vertical displacement rates presented in Fig. 3 show large differences across Yangon City, ranging from −110 mm/yr up to +11 mm/yr. Even though the results still contain small uncertainties, the errors of individual PS should not be larger than a few mm/yr as 33 images were used in the PSI analysis. The mean root mean square error of 3.5 mm/yr should give an approximation of the error introduced. The area with little to no measured vertical deformation velocity coincides with the geology map layers of the tertiary age shown in Fig. 6 which are expected to show few signs of motion. In other words, the presented velocity rates are relative to the motion of the Shwedagon-Mingaladon anticlinal ridge shown in the same figure. Assuming that the majority of the measured deformation is composed of surface movement, the negative deformation velocity values in Fig. 3 point to subsidence.

The previous work by Aobpaet et al. (2014) already points to displacement at site A, but in this research also three additional sites (B–D) with relative movement over 20 mm/yr were discovered. The comparison of the average velocity magnitude at site A between both studies does not show large differences, but a larger area was measured in this study because more scattering objects have been added over time.

5.2. Likely explanations of deformation

A comparison of the vertical deformation with the geology map of Yangon, presented in Fig. 6, suggests that the areas with alluvial and valley filled deposits are highly susceptible to rapid vertical motion since 95% of deformation rates over 10 mm/yr are found over deposits of the Quaternary age. Moreover, all selected sites A through D are located over the young alluvium deposits. The valley west of the major anticlinal ridge in Yangon is filled with unconsolidated alluvium deposits ranging in thickness from a few feet near the ridge to about 70 to

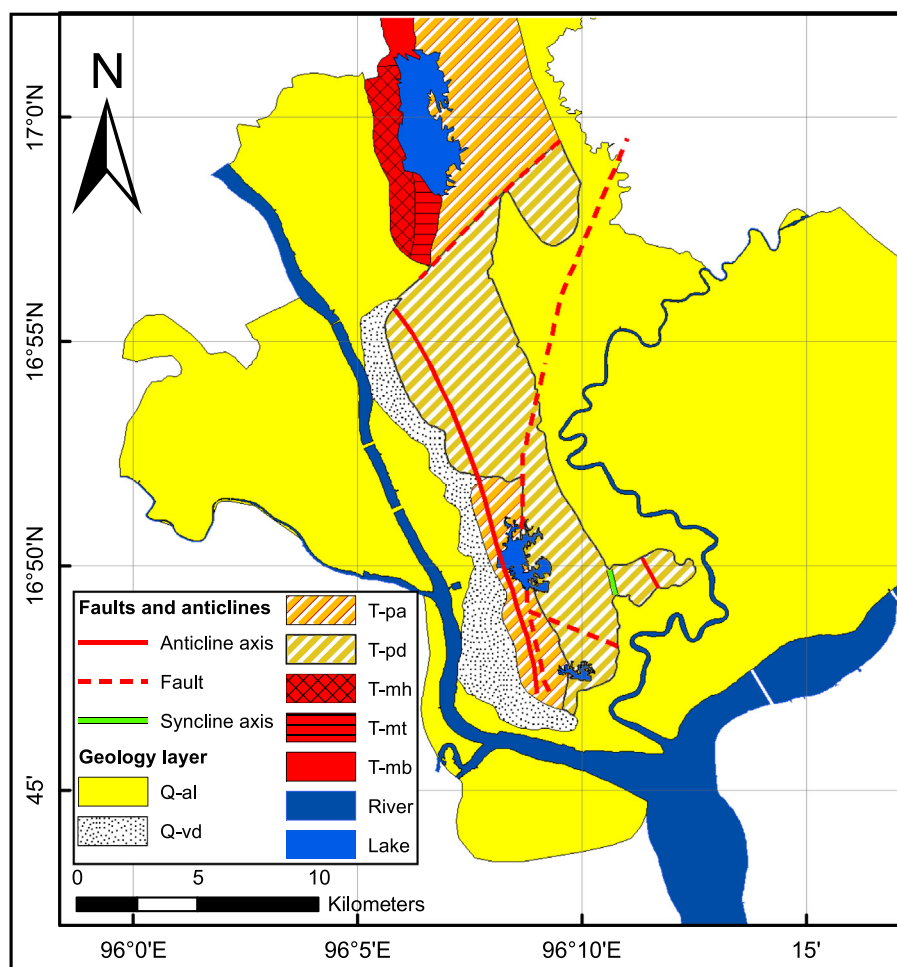


Fig. 6. Geology map of Yangon after Naing (1972) upgraded by the Water Resources Utilization Department. The map shows a large extent of Quaternary age deposits, young alluvium (Q-al) and valley filled deposits (Q-vd). The deposits of the Tertiary age consist of Danyingon clays (T-pd) and Azarnigon sandrocks (T-pa) of the Irrawaddy Formation (Pliocene) and Besapet alternation (T-mb), Thadugan sandstones (T-mt), and Hlawga shales (T-mh) of the Pegu Group (Miocene). The Tertiary deposits are mainly found on the Shwedagon-Mingaladon anticlinal ridge, at 6 to 25 m higher in elevation than the Quaternary deposits.

100 m in the valley (Wai, 2016). When one compares this description with the deformation rates at site B shown in Fig. 3, an increasing downward velocity was found to the west of the ridge. This indicates that the rate of deformation is likely also dependent on the thickness of the Quaternary deposit layers.

The load increase on top of the soil in Yangon mainly consists of roads, houses, and industries. Analysis of the PSI results showed that the most rapid vertical motion nearly always coincides with recent constructions. In this research, closer inspection was performed over the expansion of three industrial zones in Yangon. Fig. 4 shows a relation between the age of construction and the vertical displacement velocity of the measured objects in the first years of construction. Little change in the average vertical velocity is observed at buildings constructed over 10 years before the start of the measurement. Therefore, the load increase on top of Yangon can be used to explain the most severe vertical deformation peaks found throughout the city that can differ from 10 up to 50 mm/yr between neighboring pixels.

Average vertical deformation velocity of the 2004 epoch—not caused by a load increase—was approximately 40 mm/yr at site A, between 15 and 20 mm/yr at site B. At site C, recent surface cover change is only observed with the expansion of the Ahlone township harbor at the riverside, but the most severe deformation centered around 20 mm/yr is found more towards the north where the surface cover remained unchanged over the past decades. The surface cover at site D also remained virtually unchanged over the past two decades,

which means that there is another cause for the surface to move down at rates between –20 and 25 mm/yr for that location.

Fig. 5 shows that the estimated rate of groundwater extraction at sites A–D greatly exceeds the expected rate of groundwater recharge from the surface. The values stated here are based on several assumptions and may have been either over- or underestimated. Moreover, extraction of industrial water was not taken into account. To make an estimate of industrial water usage, an attempt was made to retrieve extraction permits that were issued in the areas of interest. However, the department of Urban&Housing development of the Ministry of Construction, responsible for issuing the permits for groundwater extraction, indicated that the majority of groundwater extractions occurs illegally without an issued permit (pers. comm. Thi Thi Khaing, 15 Aug 2017). Nevertheless, the current estimates are deemed accurate enough to display domestic water usage with a relative accuracy of 12%.

In Fig. 7, the relation is shown between the change potential in water storage and the average subsidence rate measured at structures built over 10 years before the measurement (where the motion of scatterers and the surface is assumed to be equal). Each point in this figure represents a single township. A distinction in geologic age has been made (Quaternary and Tertiary) to separately assess the relation of subsidence to groundwater extraction. Change potential in water storage has a Pearson correlation of 0.86 with the vertical subsidence rate for the Quaternary extraction when the outliers are not taken into account. This shows that subsidence in these areas is likely caused by

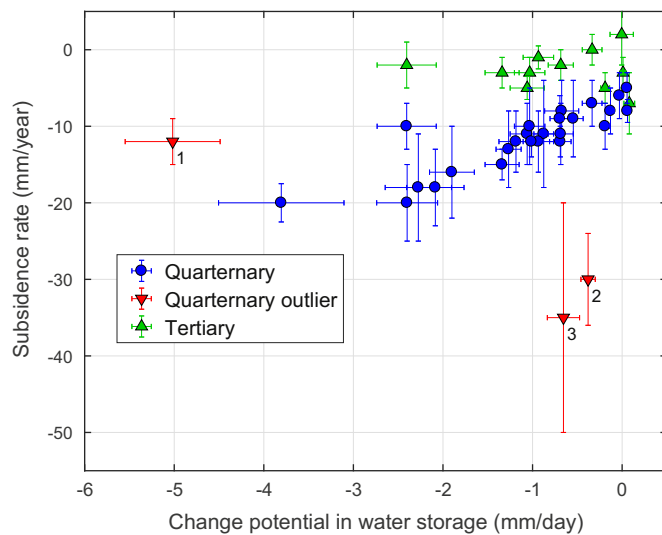


Fig. 7. Scatter-plots showing estimated change potential in water storage versus average subsidence rate for each township. Three classifications are used: Quaternary geology layers in blue circles, Quaternary geology outliers as red triangles pointing down each marked with a number, and Tertiary geology layers in green triangles pointing up. Partial Tertiary and Quaternary areas within the same township were assessed separately on subsidence rate. The most important relation is found in Quaternary townships where groundwater extraction and subsidence are positively correlated with a Pearson correlation coefficient of 0.86. The horizontal and vertical error-bars denote the $\pm 1\sigma$ range.

groundwater extraction. The Tertiary layers show no correlation with change in water storage potential which can be explained by the fact that these soil layers are generally well consolidated. Moreover, Tertiary layers contain fewer extraction points when comparing the YCDC pump locations in Fig. 2 with the geology map in Fig. 6.

The townships with little to no groundwater extraction shown in Fig. 7 still show some subsidence in the range of -10 to 0 mm/yr. This is partially explained by natural subsidence which is typically in the order of 1 – 4 mm/yr (Syvitski et al., 2009) and found stronger in

Quaternary age deposits than Tertiary age deposits. Also, settling of the measured objects might contribute several millimeters per year to the subsidence measurement. Finally, the deformation values are relative to a reference point which might not be stationary with respect to a geodetic datum.

In the Quaternary age category, there are three distinct outliers that do not clearly satisfy the extraction-subsidence relation found at the other townships. The outlier marked with 1 points to the Sanchaung township—not located in zones A through D—and the outliers marked with 2 and 3 correspond to the townships Dagon Myothit North and East, both located in zone A. Although the township outliers marked with 2 and 3 show a wide range of subsidence rates within the township, the precision of the individual measurement is in the order of 3 mm/yr. The estimation of the change in water storage potential, however, is more likely to contain errors or misrepresent the physical reality.

The outlier marked with 1 was estimated at 5 mm/day which could easily be an over-estimation, but it is even more likely that the full potential can never be reached as horizontal inflow prevents further draw-down of the groundwater level. The domestic groundwater extraction estimations at outlier 2 and 3 seem far too low to satisfy the Quaternary subsidence-extraction relation. There are several facts that could help explain this mismatch. Firstly, the screens of the YCDC operated wells are placed between 100 and 150 m, so water is less easily recharged to the deeper aquifers which makes it more likely that the full change potential in water storage is reached. Secondly, there is a large industrial zone located in the center of zone A which is not in proximity to any surface water (Fig. 1). Large industrial groundwater extractions could explain the high subsidence rates found here, though there is no data to support this claim. Lastly, as zone A concerns a recent expansion of Yangon city, increasing effective stresses in the soil is more likely to exceed historical values than in older parts of Yangon.

In zone A at Dagon University, signs were found that the soil moved down more rapidly than the building as shown in Fig. 8. This might be more related to drainage of the top layer of the soil, rather than groundwater extraction which typically occurs beneath the foundation layers of constructed buildings. Drainage in the top layer of the soil could induce oxidation of organic material such as found by Cuenca and Hanssen (2008) and Morishita and Hanssen (2015) in the Netherlands.



Fig. 8. Damage found at the administration building of Dagon University, likely caused by subsidence originating from layers above the foundation zone of the building. Dagon University is located at the North side of the subsidence zone marked with A. The PS near and over the building indicate subsidence rates near 45 mm/yr, and the building was constructed in 2005.

If this were the case, one would also expect a strong seasonal pattern in the temporal behavior of subsidence.

5.3. Unrelated to deformation

Because of the severe seasonal behavior of Yangon's climate, it is possible that the surface deformation could also show signs of a seasonal signal such as found in other studies (Morishita and Hanssen, 2015; North et al., 2017; Gahalaut et al., 2017). For instance, the recharge flux varies significantly throughout the year causing changes in phreatic water level, or decomposition of organic matter in the dry season could affect deformation velocity. To assess the impact of a seasonal signal, the PSI time-series were analyzed for periodical deformation superimposed on the steady-state deformation model as done before by Cuenca and Hanssen (2008). This analysis did, however, not result in significant seasonality patterns for Yangon city as less than 0.1% of the PS shows a superimposed amplitude over 4.5 mm for a sine with a period of 1 year. These points were scattered around the city rather than being concentrated in zones and are mostly in-phase with the cloud cover (moving up and down during the dry and rainy season respectively). Only very few points were in-phase with soil moisture conditions (moving down and up during the dry and rainy season respectively). This suggests that subsidence is not closely related to the phreatic water level.

5.4. Potential impact

It appears evident that current rates of groundwater extraction are unsustainable as they result in subsidence rates that are largely caused by the extraction of groundwater. Similar cases in surrounding countries have led to serious consequences of subsidence such as in Bangkok where severe overexploitation of groundwater resulted in areas sinking up to 1.0 m below the mean sea level which has drastically increased the risk of flooding events (Phien-wej et al., 2006). Current and future infrastructure needs to be adapted to withstand differential settlements such as with the development of new MRT lines in Ho Chi Minh City (Thoang and Giao, 2015) or the hampered development of sustainable economic zones in the Hong Kong environment (Chen et al., 2012). Finally, degradation of the aquifer system poses challenges for future water availability like in the Rafsanjan plain (Motagh et al., 2017).

The previous cases exemplify the potential consequences for Yangon as similar subsidence rates were found and comparable conditions are met. Flooding events already occur frequently (JICA, 2014b) so an increase in frequency and severity can be expected. The aquifer system is compacting as indicated by the volume loss found in this research. On top of that, saline water has intruded into Yangon's aquifers (Htun, 2015) which endangers future groundwater extractions for domestic use. We argue that groundwater extractions in Yangon must be mitigated similarly as done in Bangkok (Phien-wej et al., 2006) to stop land subsidence and to ensure future availability of ground water resources.

6. Conclusion

Using the PSI results, we were able to show that half of Yangon is subsiding at rates over 10 mm/yr in the period of December 2014 until April 2017. In this period, a storage volume of 13 million cubic meters in the aquifer system was lost. Four sites with severe subsidence velocities over 20 mm/yr were identified at an extent of 15% of all data points. The two largest and most dominant of these sites were found at former agricultural areas where the city has expanded into over the past three decades.

Subsidence potential of the soil is high in deposits of Quaternary age as the presence of Quaternary geology layers accounts for 95% of all measured subsidence rates over 10 mm/yr. The rates of subsidence presented in this research are far higher than typical rates of natural subsidence, which shows that the human influence on subsidence is

dominant. The two driving forces that explain the subsidence patterns are the addition of loads on top of the surface, and the extraction of groundwater from the subsoil. Loads on the soil, in the form of roads, buildings, and industries, affect the subsidence velocities mostly in the first decade after placement. The measured deformation over these structures exceeds neighboring velocities by 10 to 20 mm/yr, but this difference is negligible after a period of 10 years. The subsidence, originating from scatterers placed over a decade before the S1 acquisitions, is largely explained by the extraction of groundwater. A strong correlation between subsidence and change in groundwater storage is found at the Quaternary age deposited layers. An exception to this relation holds for three townships where the estimates might not reflect the physical reality and where other unidentified causes may also contribute to subsidence.

We argue that the current operation of groundwater extractions is unsustainable as it results in depleting and degrading aquifers as is evident by the land subsidence found over Yangon. The strong correlation between the extracted amounts of groundwater and subsidence rates shows that mitigation of groundwater usage is key to reducing subsidence rates over time.

Acknowledgments

This work was strongly supported by the PSI results generated by SkyGeo (<http://www.skygeo.com>) for the Parters-for-Water project financed by the Netherlands Enterprise Agency. Furthermore, the authors are grateful to the water and sanitation engineers at YCDC who were kind enough to share their data on tube wells. Also many thanks to professors Kyaw Aung and Tun Naing of Yangon Technological University for sharing their data and research on the Geology of Yangon. A final word of thanks goes out to Dr. Win Min Oo who helped with translations and other support for this research.

References

- Aobpaet, A., Trisirisatayawong, I., Aung, H.H., Maksin, P., Space Technology Development Agency, Myanmar Earthquake Committee, Persistent Scatterer Insar, 2014. Yangon surface displacement as detected by InSAR time series. In: Asian Association on Remote Sensing, pp. 1–6.
- Berger, M., Moreno, J., Johannessen, J.A., Levelt, P.F., Hanssen, R.F., 2012. ESA's Sentinel missions in support of Earth system science. *Remote Sens. Environ.* 120, 84–90.
- Chai, J.-C., Shen, S.-L., Zhu, H.-H., Zhang, X.-L., 2004. Land subsidence due to groundwater drawdown in Shanghai. *Géotechnique* 54 (2), 143–147. <https://doi.org/10.1680/geot.54.2.143.36332>.
- Chen, F., Lin, H., Zhang, Y., Lu, Z., 2012. Ground subsidence geo-hazards induced by rapid urbanization: implications from InSAR observation and geological analysis. *Nat. Hazards Earth Syst. Sci.* 12 (4), 935–942.
- Cuenca, M.C., Hanssen, R., 2008. Subsidence due to peat decomposition in the Netherlands, kinematic observations from radar interferometry. *Eur. Space Agency Spec. Publ. ESA SP(649 SP)*. <https://www.scopus.com/inward/record.uri?eid=2-s2.0-47249148769&partnerID=40&md5=98bebe8e066246cd52862e5c66d9dfeb>.
- Department of Population, 2015. The 2014 Myanmar Population and Housing Census Yangon Region. In: Tech. Rep. Ministry of Immigration and Population (May).
- Ferretti, A., Prati, C., Rocca, F., 2000. Nonlinear subsidence rate estimation using permanent scatterers in differential SAR interferometry. *IEEE Trans. Geosci. Remote Sens.* 38 (5), 2202–2212.
- Ferretti, A., Prati, C., Rocca, F., 2001. Permanent scatterers in SAR interferometry. *IEEE Trans. Geosci. Remote Sens.* 39 (1), 8–20.
- Gahalaut, V.K., Yadav, R.K., Sreejith, K.M., Gahalaut, K., Bürgmann, R., Agrawa, R., Sati, S.P., Bansal, A., 2017. InSAR and GPS measurements of crustal deformation due to seasonal loading of Tehri reservoir in Garhwal Himalaya, India. *Geophys. J. Int.* 209 (1), 425–433.
- Galloway, D.L., Hudnut, K.W., Ingebritsen, S.E., Phillips, S.P., Peltzer, G., Rogez, F., Rosen, P.A., 1998. Detection of aquifer system compaction and land subsidence using interferometric synthetic aperture radar, Antelope Valley, Mojave Desert, California. *Water Resour. Res.* 34 (10), 2573–2585. <https://doi.org/10.1029/98WR01285>. (oct).
- Google, 2017. Google Earth Pro. <http://www.earth.google.com>.
- Hanssen, R.F., 2001. Radar Interferometry. Remote Sensing and Digital Image Processing, vol. 2 Springer Netherlands, Dordrecht. <https://doi.org/10.1007/0-306-47633-9>.
- Higgins, S.A., 2015. Review: advances in delta-subsidence research using satellite methods. *Hydrogeol. J.* 24 (3), 587–600. <https://doi.org/10.1007/s10040-015-1330-6>.
- Hooper, A., Bekaert, D., Spaans, K., Arian, M., 2012. Recent advances in SAR interferometry time series analysis for measuring crustal deformation. *Tectonophysics* 514–517, 1–13.

- Htun, W.W., 2015. Assessment of Groundwater Vulnerability in Yangon City, Myanmar. JICA, 2014. The project for the improvement of water supply, sewerage and drainage - Vol II: water supply system summary. In: Tech. rep..
- JICA, 2014. The project for the improvement of water supply, sewerage and drainage - Vol III: water supply system master plan. In: Tech. rep. JICA.
- JICA, 2014. The project for the improvement of water supply, sewerage and drainage - Vol VI: sewerage and drainage system master plan. In: Tech. rep..
- Kampes, B.M., 2005. Displacement Parameter Estimation using Permanent Scatterer Interferometry (Ph.D. thesis). TU Delft.
- Ketelaar, V., 2009. Satellite Radar Interferometry. vol. 14 Springer Netherlands, Assen.
- Kratzsch, H., 2012. Mining Subsidence Engineering. Springer Science & Business Media.
- Minderhoud, P.S.J., Erkens, G., Pham, V.H., Bui, V.T., Erban, L., Kooi, H., Stouthamer, E., 2017. Impacts of 25 years of groundwater extraction on subsidence in the Mekong delta, Vietnam. *Environ. Res. Lett.* 12 (6), 064006. <http://stacks.iop.org/1748-9326/12/i=6/a=064006?key=crossref.687693ccba9bba2f8d848aa7018a5625>.
- Mon, E.K., Htay, Y.Y., Tun, S.L., Aung, Z.W., 2013. Yangon's Water Supply Treatment Issues.
- Morishita, Y., Hanssen, R.F., 2015. Deformation parameter estimation in low coherence areas using a multi-satellite InSAR approach. *IEEE Trans. Geosci. Remote Sens.* 53 (8), 4275–4283.
- Morley, I., 2013. Rangoon. *Cities* 31, 601–614.
- Motagh, M., Shamshiri, R., Haghshenas Haghighi, M., Wetzel, H.-U., Akbari, B., Nahavandchi, H., Roessner, S., Arabi, S., 2017. Quantifying groundwater exploitation induced subsidence in the Rafsanjan plain, southeastern Iran, using InSAR time-series and in situ measurements. *Eng. Geol.* 218, 134–151. <http://linkinghub.elsevier.com/retrieve/pii/S0013795217300789> (feb).
- Naing, W., 1972. The Hydrogeology of Greater Rangoon Area. (Msc thesis, Yangon Technological University).
- North, M., Farewell, T., Hallett, S., Bertelle, A., 2017. Monitoring the response of roads and railways to seasonal soil movement with persistent scatterers interferometry over six UK sites. *Remote Sens.* 9 (9), 922. <http://www.mdpi.com/2072-4292/9/9/922>.
- Phien-wej, N., Giao, P.H., Nutalaya, P., 2006. Land subsidence in Bangkok, Thailand. *Eng. Geol.* 82 (4), 187–201.
- RVO Netherlands, 2014. Myanmar Integrated Water Resources Management, Strategic Study.
- Samiei-Esfahany, S., Hanssen, R.F., van Thienen-Visser, K., Muntendam-Bos, A., 2010. On the Effect of Horizontal Deformation on InSAR Subsidence Estimates. In: ESA Special Publication. ESA Special Publication, vol. 677. pp. 39 (Mar).
- Sousa, J.J., Hooper, A.J., Hanssen, R.F., Bastos, L.C., Ruiz, A.M., 2011. Persistent scatterer InSAR: a comparison of methodologies based on a model of temporal deformation vs. spatial correlation selection criteria. *Remote Sens. Environ.* 115 (10), 2652–2663. <https://doi.org/10.1016/j.rse.2011.05.021>.
- Syvitski, J.P.M., 2008. Deltas at risk. *Sustain. Sci.* 3 (1), 23–32.
- Syvitski, J.P.M., Kettner, A.J., Overeem, I., Hutton, E.W.H., Hannon, M.T., Brakenridge, G.R., Day, J., Vörösmarty, C., Saito, Y., Giosan, L., Nicholls, R.J., 2009. Sinking deltas due to human activities. *Nat. Geosci.* 2 (10), 681–686. <https://doi.org/10.1038/ngeo629>. (oct).
- Thoang, T.T., Giao, P.H., 2015. Subsurface characterization and prediction of land subsidence for HCM City, Vietnam. *Eng. Geol.* 199, 107–124. <https://doi.org/10.1016/j.enggeo.2015.10.009>.
- Van Leijen, F.J., 2014. Persistent Scatterer Interferometry based on Geodetic Estimation Theory (Ph.D. thesis). Delft University of Technology.
- Verruijt, A., 2012. Soil Mechanics. Delft University of Technology. <http://geo.verruijt.net/>.
- Wai, M., 2016. Engineering Geological Subsurface Exploration Using Standard Penetration Test and Cone Penetration Test for Mayangone and Hlaing townships. Msc.
- Wang, F., Miao, L., Lu, W., 2013. Sand creep as a factor in land subsidence during groundwater level recovery in the southern Yangtze River delta, China. *Bull. Eng. Geol. Environ.* 72 (3–4), 273–283.
- Wegmuller, U., Werner, C., Strozzi, T., Wiesmann, A., Frey, O., Santoro, M., 2015. Sentinel-1 IWS mode support in the GAMMA software. In: 2015 IEEE 5th Asia-Pacific Conference on Synthetic Aperture Radar (APSAR). IEEE, pp. 431–436. <http://ieeexplore.ieee.org/document/7306242/> sep.
- YCDC, 2015. Situation of water supply system of Yangon City and it's future demand. In: Tech. rep. YCDC.